

Investigating Vibration Properties of a Planetary Gear Set with a Cracked Tooth in a Planet Gear

Xihui Liang¹ and Ming J. Zuo²

^{1,2}*Department of Mechanical Engineering, University of Alberta, Edmonton, Alberta, T6G2G8, Canada
ming.zuo@ualberta.ca*

ABSTRACT

Comparing with fixed shaft gearbox, vibration properties of planetary gearbox are much more complicated. In a planetary gearbox, there are multiple vibration sources as several pairs of sun-planet gears and several pairs of ring-planet gears mesh simultaneously. In addition, the signal transmission path changes due to the rotation of the carrier. To facilitate fault detection of a planetary gearbox and avoid catastrophic consequences caused by gear failures, it is essential to understand the vibration properties of a planetary gearbox. This paper aims to simulate vibration signals and investigate vibration properties of a planetary gear set when there is a cracked tooth in a planet gear. Displacement signals of the sun gear and the planet gear, and resultant acceleration signals of the whole planetary gear set will be simulated and investigated. Previous work mainly focuses on the vibration properties of a single component, like the sun gear, the planet gear or the carrier. This paper simulated the vibration signal of a whole planetary gear set when there is a cracked tooth in a planet gear. In addition, fault symptoms will be revealed, which can be utilized to detect the crack in the planet gear. Finally, the proposed approach is experimentally validated.

1. INTRODUCTION

Planetary gears are widely used in aeronautic and industrial applications because of properties of compactness and high torque-to-weight ratio. A planetary gear set consists normally of a centrally pivoted sun gear, a ring gear and several planet gears that mesh with the sun gear and the ring gear simultaneously as shown in Figure 1.

The vibration signals of a planetary gearbox are more complicated comparing with that of a fixed-shaft gearbox. In a planetary gearbox, there are multiple vibration sources as several pairs of sun-planet gears and several pairs of ring-

planet gears mesh simultaneously. In addition, signal transmission path changes due to the rotation of the carrier. Multiple vibration sources and the effect of transmission path lead to complexity of fault detection (Liang, Zuo and Hoseini, 2014).

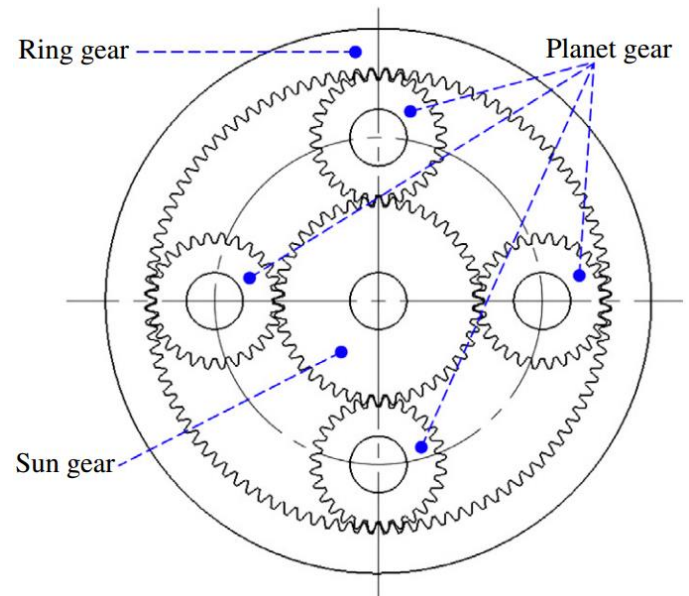


Figure 1. A planetary gear set having four planet gears (Lei, Lin, Zuo and He, 2014)

A few studies investigated vibration properties of the planetary gearbox. Zhang, Khawaja, Patrick, et al. (2008) applied the blind deconvolution algorithms to denoise the vibration signals collected from a testbed of the helicopter main gearbox subjected to a seeded fault. Inalpolat and Kahraman (2009) proposed a simplified mathematical model to describe the mechanisms leading to modulation sidebands of planetary gear sets. Inalpolat and Kahraman (2010) predicted modulation sidebands of a planetary gear set having manufacturing errors. Chen, Vachtsevanos and Orchard (2012) proposed an integrated remaining useful life prediction method which was validated by successfully applying the method to a seeded fault test for a UH-60 helicopter planetary gear plate. Feng and Zuo (2012)

Xihui Liang et al. This is an open-access article distributed under the terms of the Creative Commons Attribution 3.0 United States License, which permits unrestricted use, distribution, and reproduction in any medium, provided the original author and source are credited.

mathematically modeled tooth pitting and tooth wear by applying amplitude modulation and frequency modulation, and then analyzed the spectral structure of the vibration signals of a planetary gear set. Patrick, Ferri and Vachtsevanos (2012) studied the effect of planetary gear carrier-plate cracks on vibration spectrum. Liang, Zuo and Hoseini (2014) investigated the vibration properties of a planetary gear set when there is a cracked tooth in the sun gear. Chen and Shao (2011) studied the dynamic features of a planetary gear set with tooth crack under different sizes and inclination angles. The displacement signals of the sun gear and the planet gear were investigated when a tooth crack was present on the sun gear or the planet gear. However, the effect of transmission path was not considered in their analysis. They did not model the resultant vibration signals of the whole gearbox. In practical applications, sensors are commonly mounted on the housing of the gearbox to capture the vibration signals. The signals acquired by sensors are the resultant vibration signals of the whole gearbox. They are not the vibration signals of the sun gear or a single planet gear. In this study, the resultant vibration signals of a planetary gear set will be modeled and then analyzed when there is a cracked tooth in the planet gear.

2. MODELING OF VIBRATION SIGNALS

Liang, Zuo and Hoseini (2014) simulated and investigated the vibration signals of a planetary gear set when there is a cracked tooth in the sun gear. The method proposed by Liang, Zuo and Hoseini (2014) will be applied directly in this paper. This study does not intend to propose a new method to model the vibration signals of a planetary gear set. This paper focuses on exploring vibration properties, and then finds the fault symptoms of a planetary gear set when there is a cracked tooth in the planet gear. Two steps are required to obtain the resultant vibration signals of a planetary gear set. First of all, a dynamic model will be applied to simulate the vibration signals of each gear, including the sun gear, each planet gear and the ring gear. Then, resultant vibration signals will be modeled considering multiple vibration sources and effect of transmission path.

2.1. Dynamic Modeling of a Planetary Gear Set

The dynamic model used in this study is the same as that used by Liang, Zuo and Hoseini (2014) except for differences of sun-planet mesh stiffness. The differences of sun-planet mesh stiffness will be described in detail in Section 3. Figure 2 shows the dynamic model that will be used in this study. It is a nonlinear two-dimensional lumped-mass model. Each component has three degrees of freedom. Total, it has $9+3N$ degrees of freedom as a planet gear set has one sun gear, one ring gear, one carrier and N planet gears. All the coordinate systems are fixed on the carrier. Figure 2 shows locations and positions of all coordinate

systems in the initial time (time zero). Equations of motion of the dynamic model will not be included in this paper. Equations can be found in Liang, Zuo and Hoseini (2014).

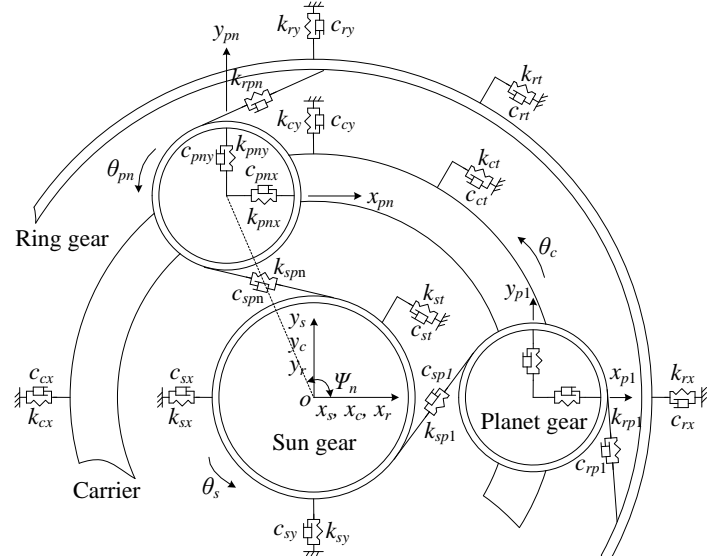


Figure 2. Dynamic modeling of a planetary gear set (Liang, Zuo and Hoseini, 2014)

2.2. Resultant Vibration Signals

A dynamic model of a planetary gear set was described in Section 2.1. Equations of motion of the dynamic model can be built correspondingly. Numerically solving the equations, vibration signals of the sun gear, the ring gear, each planet gear and the carrier can be obtained. After that, resultant vibration signal of the planetary gear set can be modeled incorporating multiple vibration sources and the effect of transmission path. The resultant vibration signal is expressed as weighted summation of acceleration of each planet gear as shown in Equation (1) (Liang, Zuo and Hoseini, 2014).

$$a(t) = \sum_{n=1}^N w_n(t) a_n(t) \quad (1)$$

where $w_n(t)$ is the weighting function which counts for the effect of the transmission path; $a_n(t)$ represents acceleration of the n^{th} planet gear, which is obtained through dynamic simulation.

A Hamming function is used to model the effect of transmission path. The Hamming function assumes that as planet n approaches transducer location, its influence increases, reaching its maximum when planet n is closest to transducer location, then, its influence decreases as the planet goes away from the transducer.

$$w_i(t) = 0.54 - 0.46 \cos(w_c t + \psi_n) \quad (2)$$

where w_c is carrier angular frequency; ψ_n is phase angle corresponding to the n^{th} planet gear.

3. CRACK MODELING AND MESH STIFFNESS EVALUATION

Gear tooth crack is a common failure mode in a gear transmission system. It may occur in the sun gear, a planet gear or the ring gear. When a cracked tooth is in the sun gear, the cracked tooth will mesh with all planet gears. Therefore, mesh stiffness of all sun-planet gear pairs will be affected. While if a cracked tooth is in a planet gear, only mesh stiffness of one pair of sun-planet gear pair is affected.

Tooth crack mostly initiates at the critical area of a gear tooth root (area of the maximum principle stress), and the propagation paths are smooth, continuous, and in most cases, rather straight with only a slight curvature as shown in Figure 3 (Belsak and Flasker, 2007). Liang, Zuo and Pandey simplified the crack growth path as a straight line (the red line) starting from the critical area of the tooth root. The same model developed by Liang, Zuo and Pandey (2014) will be applied in this study.

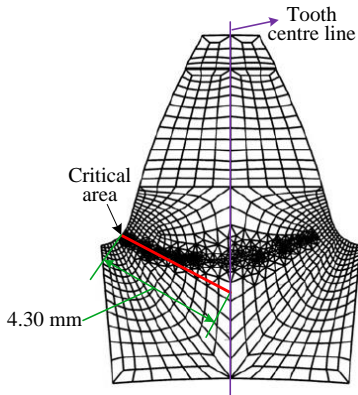


Figure 3. Crack propagation path (Belsak and Flasker, 2007)

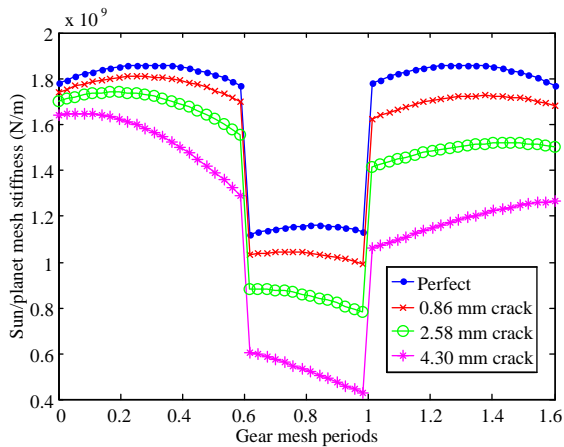


Figure 4. Mesh stiffness of a sun-planet gear pair (Liang, Zuo and Pandey, 2014)

Potential energy method used by Liang, Zuo and Pandey (2014) is applied directly in this study to evaluate the mesh stiffness of a planetary gear set in the perfect and the cracked tooth condition. Figure 4 shows the mesh stiffness

of a pair of sun-planet gear when different crack levels are present on a planet gear tooth. With the growth of tooth crack, the mesh stiffness will decrease correspondingly. The reduction of mesh stiffness will cause the vibration signals behavior abnormally, which can be used to detect the tooth fault.

4. VIBRATION SIGNALS OF SUN GEAR AND PLANET GEAR

In this section, vibration signals of a planetary gear set are numerically simulated using MATLAB ode15s solver. Physical parameters of the planetary gear set are listed in Table 1. A constant torque of 450 N.m is applied to the sun gear and the rotation speed of the carrier is 8.87 r/min. Gear mesh damping is assumed to be proportional to the mesh stiffness (Tian, Zuo and Fyfe, 2004).

Table 1. Physical parameters of a planetary gear set (Liang, Zuo and Hoseini, 2014)

Parameters	Sun gear	Planet gear	Ring gear	Carrier
Number of teeth	19	31	81	---
Module (mm)	3.2	3.2	3.2	---
Pressure angle	20°	20°	20°	---
Mass (kg)	0.700	1.822	5.982	10.000
Face width (m)	0.0381	0.0381	0.0381	---
Young's modulus	2.068×10^{11}	2.068×10^{11}	2.068×10^{11}	---
Poisson's ratio	0.3	0.3	0.3	---
Base circle radius	28.3	46.2	120.8	---
Root circle radius	26.2	45.2	132.6	---
Bearing Stiffness	$k_{sx} = k_{sy} = k_{rx} = k_{ry} = k_{cx} = k_{cy} = k_{pmx} = k_{pmy} = 1.0 \times 10^8 \text{ N/m}$			
Bearing damping	$c_{sx} = c_{sy} = c_{rx} = c_{ry} = c_{cx} = c_{cy} = c_{pmx} = c_{pmy} = 1.5 \times 10^3 \text{ Ns/m}$			

Figure 5 presents displacement signals of the planet gear that has a cracked tooth. The planet gear has 31 teeth. In the time duration of 31 gear mesh periods, the cracked tooth will mesh one time. It is observable from Figure 5 that large amplitude (fault symptom) of the displacement signal is generated when the cracked tooth is in meshing. As the crack grows, the amplitude of the fault symptoms increases accordingly. The fault symptom will repeat every 31 gear mesh periods. In Figure 5, the fault symptom mainly appears in the y-direction displacement. Actually, the fault symptom may mainly appear in the x-direction displacement or in the y-direction displacement or evenly in the two directions, which depends on the location of the planet gear.

Since the ring gear has 81 teeth, the planet gear returns to its original position after 81 meshes. Figure 6 plots the center locus of the sun gear in 81 gear mesh periods when a planet gear tooth has different crack lengths. When the planet gear is in perfect condition, 81 spikes can be observed which corresponding to 81 gear meshes. When the planet gear has a cracked tooth, the cracked tooth will mesh two or three times (81/31) in 81 gear mesh periods. Figure 6 shows the condition when three meshes happen in 81 gear meshes. In the condition of 0.86 mm crack, three bigger spikes can be observed. Time duration of spike 1 and spike 2 is 31 gear

mesh periods. Similarly, it is 31 gear mesh periods between spike 2 and spike 3. The time duration of spike 3 and spike 1 is 19 (81-62) gear mesh periods. It is predictable that the 4th bigger spike will show after 31 gear mesh periods of spike 3. In the condition of 2.58 mm crack, the three spikes (1, 2 and 3) become even larger comparing to the condition of 0.86 mm crack. When the cracked tooth is in meshing, a

spike will be generated due to the low stiffness of cracked tooth pair, like spike 1. Spike 1' is generated along with spike 1 by the reaction force induced by the bigger amplitude of spike 1. Same situation applies to spike 2' and spike 3'. Overall, clear fault symptoms show in the vibration signals of sun gear and planet gear.

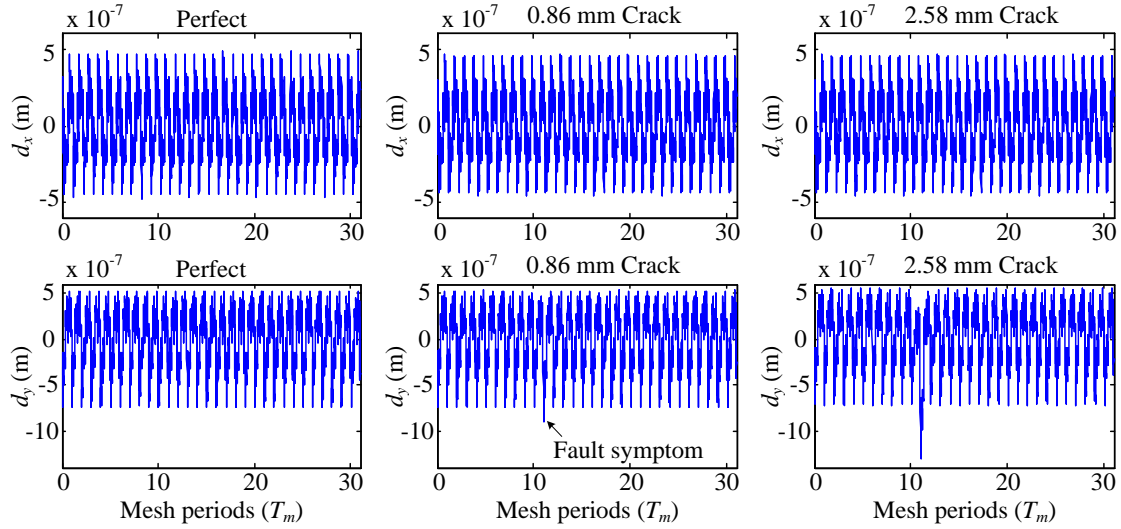


Figure 5. Displacement signals of the sun gear
 d_x : displacement in x-direction; d_y : displacement in y-direction

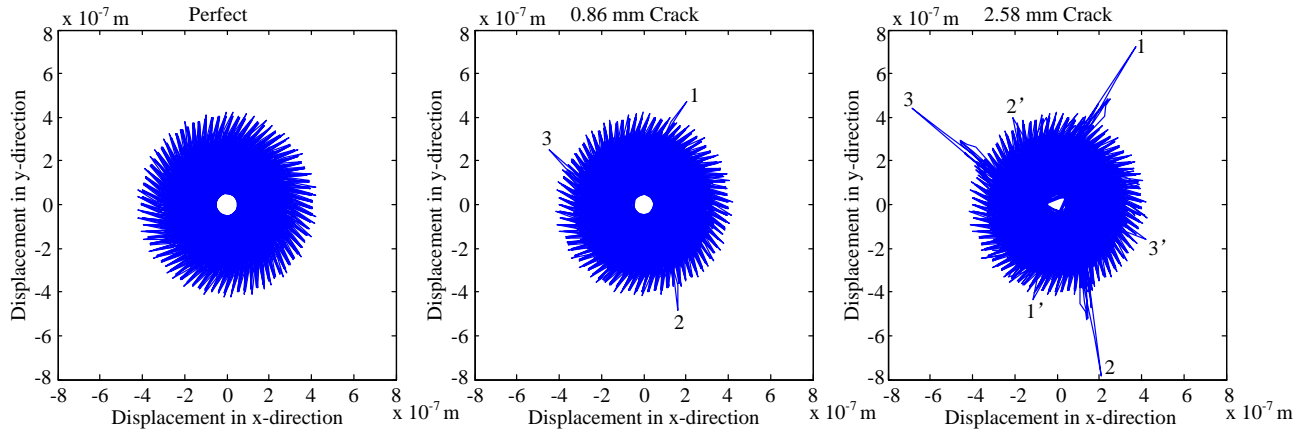


Figure 6. Center locus of the sun gear

5. RESULTANT VIBRATION SIGNALS

Applying Equation (1), resultant signal of a planetary gear set (parameters are listed in Table 1) can be generated. Figure 7 shows the resultant vibration signals in one revolution of the carrier (81 gear mesh periods). Three health conditions are plotted: perfect condition, 0.86 mm crack in one tooth of a planet gear and 2.58 mm crack in one tooth of a planet gear. The symbol a_y represents y-direction acceleration of the planetary gear set. In one revolution of the carrier, the cracked

tooth should mesh three times. Three fault symptoms should appear in one revolution of the carrier. However, in the 0.86 mm crack, only one bigger spike is observed (see the red elliptical circle). In the 2.58 mm crack, two bigger spikes are observed. Therefore, some spikes are attenuated or disappeared. This is caused by the effect of transmission path. If the cracked tooth is meshing far from a transducer, the fault symptoms cannot be acquired by the transducer. Figure 8 presents frequency spectrum of simulated resultant vibration signals of a planetary gear set in different health conditions. In the perfect condition, sizable amplitudes are marked in Figure

8 and they all show in the following locations: nf_m if n is an integer and a multiple of 4, $nf_m \pm f_c$ if n is an odd integer, $nf_m \pm 2f_c$ if n is an even integer but not a multiple of 4 (Liang, Zuo and Hoseini, 2014), where f_m represents gear mesh frequency and f_c denotes rotation frequency of the carrier. When crack is

present on one tooth of a planet gear, these sizable amplitudes are rarely affected. Some sidebands (see the area circled by red lines) appear due to the tooth crack even it is not obvious in Figure 8.

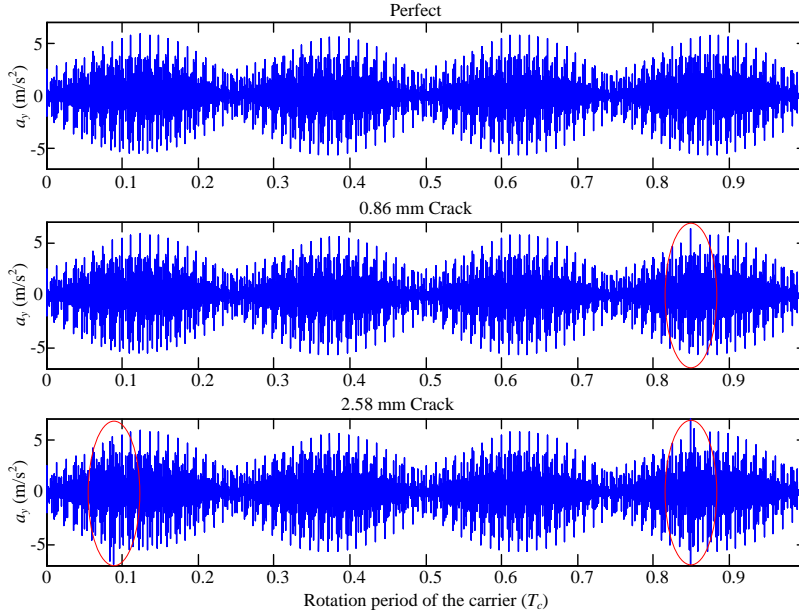


Figure 7. Simulated resultant vibration signal of a planetary gear set

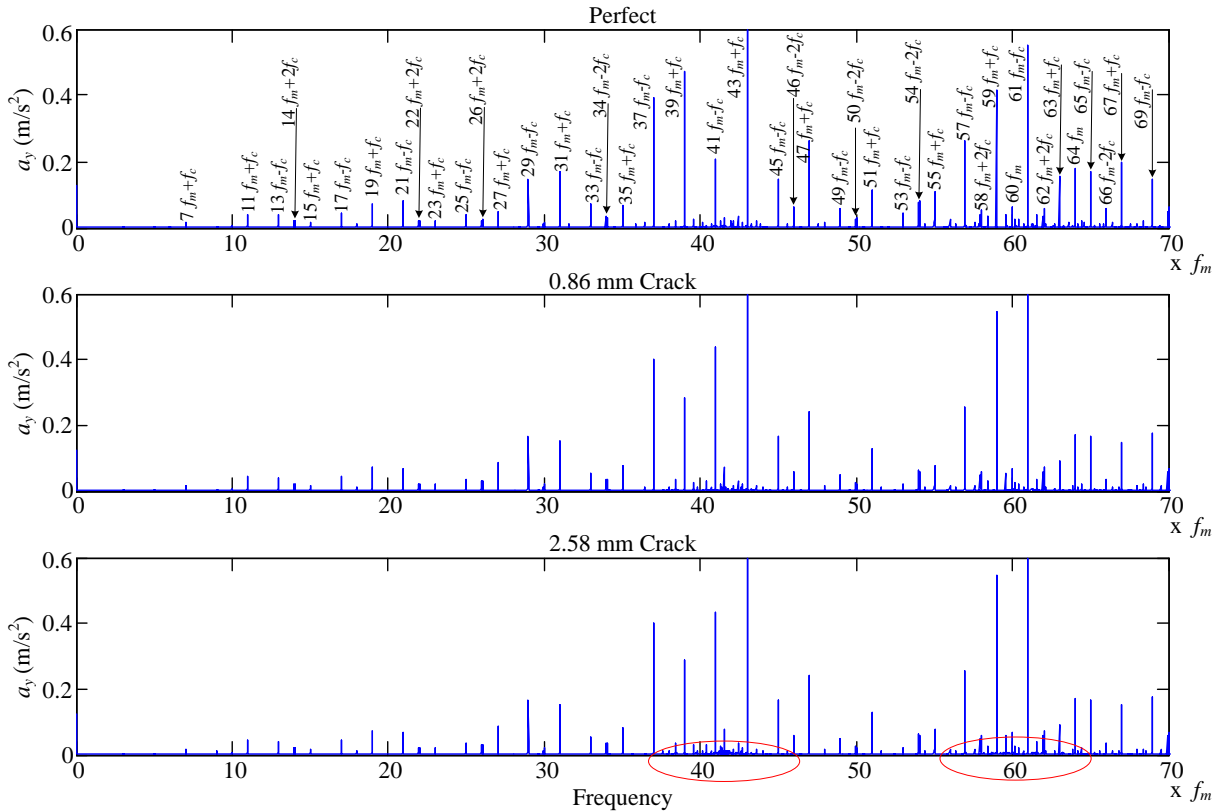


Figure 8. Frequency spectrum of simulated resultant vibration signals

Figure 9 gives zoomed-in plot of frequency region between $43 f_m$ and $45 f_m$. Many sidebands appear but they are not symmetric. Sizable sidebands appear at $m f_m \pm n f_{planet} \pm k f_c$ or $m f_m \pm n f_{planet} \pm k f_p$, where m, n and k are all integers; f_p represents rotation frequency of the planet gear and f_{planet} denotes characteristic frequency of the faulty planet gear. For the

planetary gear set we used in this studied, n and k can take the following integer values: $0 \leq n \leq 15$ and $0 \leq k \leq 1$. The characteristic frequency of the cracked planet gear can be calculated as follows (Feng et al. 2012):

$$f_{planet} = f_m / Z_p \tag{3}$$

where Z_p denotes the teeth number of the planet gear.

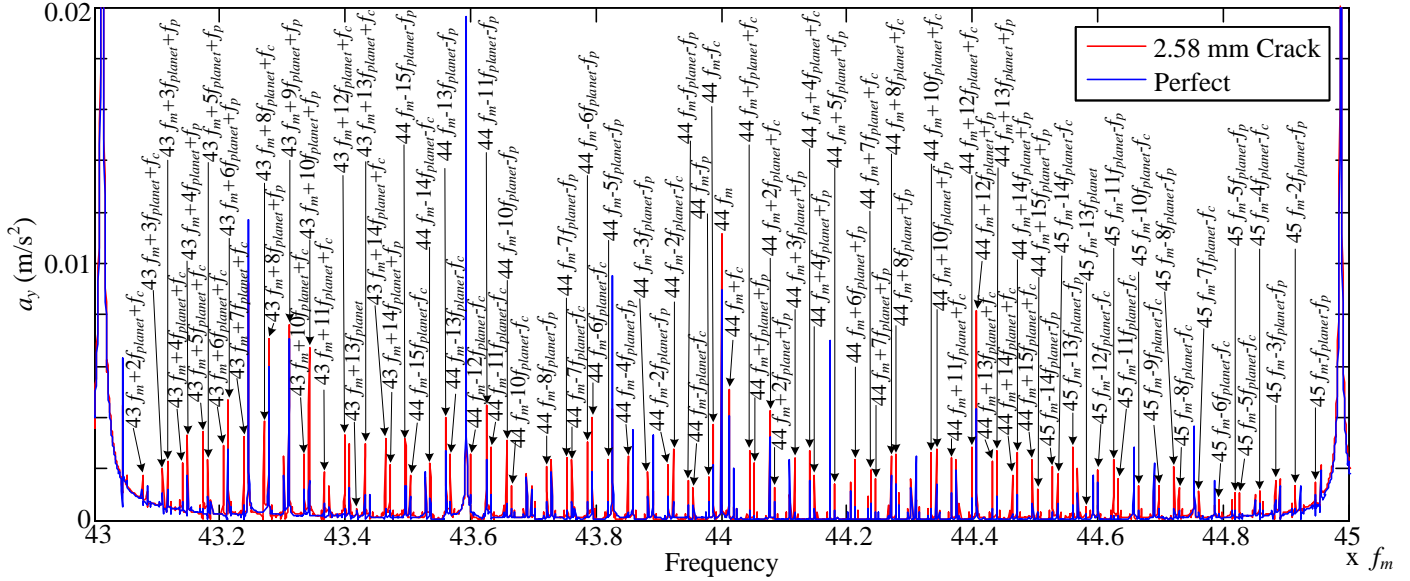


Figure 9. Zoomed-in frequency spectrum of simulated resultant vibration signals

6. EXPERIMENTAL VALIDATION

Acceleration signals are acquired from a planetary gearbox to validate simulated resultant vibration signals and fault symptoms discovered in this study. Figure 10 shows the experimental test rig whose parameters are listed in Table 2. An acceleration sensor was installed on top surface of the housing of 2nd stage planetary gearbox and vertical acceleration signals of the gearbox were recorded. The configuration and parameters of the 2nd stage planetary gear set are the same as that of the planetary gear set used for the signal simulation. The rotation speed of the carrier is 8.87 r/min that is the same carrier speed used in the simulation. When the crack length is small, fault symptoms may be submerged in the noise and hard to be detected. To amplify the fault symptoms, 4.3 mm tooth crack was created in a planet gear tooth as shown in Figure 11.

Table 2. Parameters of experimental test rig

Gearbox	Bevel stage		First stage planetary			Second stage		
	Input	Output	Sun	Planet	Ring	Sun	Planet	Ring
No. of	18	72	28	62 (4)	152	19	31 (4)	81

Note: The number of planet gears is indicated in the parenthesis.

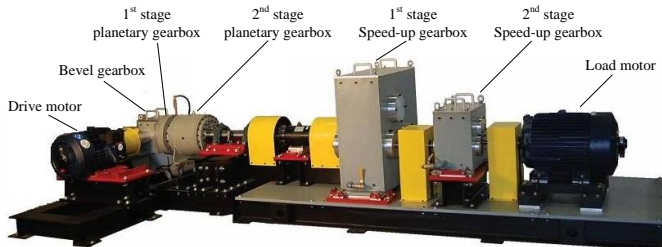


Figure 10. Experimental test rig



Figure 11. 4.3 mm manually made tooth crack in planet gear

Figure 12 shows the frequency spectrum of experimental vibration signals. In Figure 12, “Motor” represents rotation frequency of drive motor; “MBv1” denotes mesh frequency of bevel gears; “ f_{m1} ” and “ f_{c1} ” means mesh frequency and carrier

rotation frequency of 1st stage planetary gearbox, respectively. These frequencies are not relevant to the 2nd stage planetary gearbox. All other marked frequency components located at the following locations: nf_m if n is an integer and a multiple of 4, $nf_m \pm f_c$ if n is an odd integer, $nf_m \pm 2f_c$ if n is an even integer but not a multiple of 4.

Figure 13 describes frequency components of the experimental signal in the frequency region from $43 f_m$ to $45 f_m$. Sidebands are not symmetric and sizable sidebands located at $mf_m \pm nf_{planet} \pm kf_c$ or $mf_m \pm nf_{planet} \pm kf_p$, where m , n and k are all integers. The sidebands locations are the same as that anticipated in Section 5.

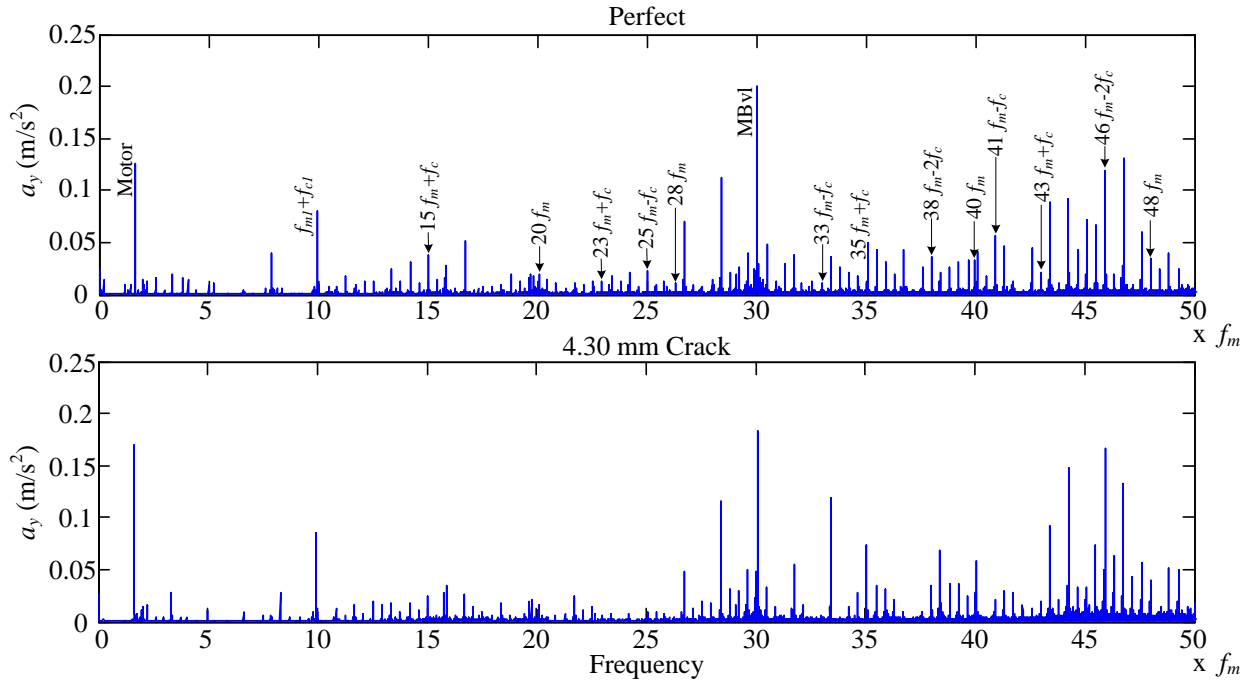


Figure 12. Frequency spectrum of experimental vibration signals

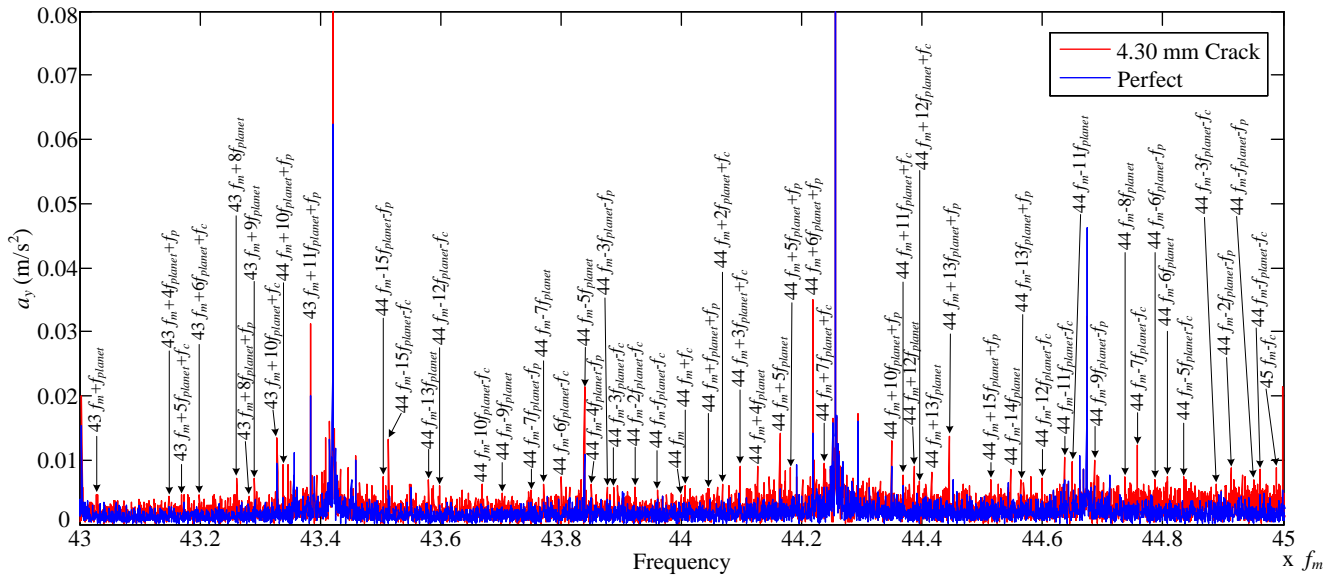


Figure 13. Zoomed-in frequency spectrum of experimental vibration signal

7. CONCLUSION

In this study, the vibration signals of a planetary gear set are simulated and investigated when there is a cracked tooth in a planet gear. When there is a cracked tooth in a planet gear, regular fault symptoms appear in the vibration signals of sun gear and planet gear. The fault symptom appears in every Z_p meshes. The fault symptoms enlarge along with the growth of crack. Some fault symptoms attenuate or disappear in the resultant vibration signal. This is due to the effect of transmission path which is caused by the rotation of carrier. Asymmetric sidebands appear when there is a cracked tooth in a planet gear. The locations of these sidebands are investigated and found, which can be used to detect tooth crack fault. Experimental validations are performed to demonstrate the correctness of the anticipated sideband locations.

ACKNOWLEDGEMENT

This research is supported by the Natural Science and Engineering Research Council of Canada (NSERC) and the China Scholarship Council (CSC).

REFERENCES

- Belsak, A., & Flaska, J. (2007). Detecting cracks in the tooth root of gears. *Engineering Failure Analysis*, vol. 14, pp. 1466-1475.
- Chen, Z., & Shao, Y. (2011). Dynamic simulation of spur gear with tooth root crack propagating along tooth width and crack depth. *Engineering Failure Analysis*, vol. 18, pp. 2149-2164.
- Feng, Z., & Zuo, M. J. (2012). Vibration signal models for fault diagnosis of planetary gearboxes. *Journal of Sound and Vibration*, vol. 331, pp. 4919-4939.
- Lei, Y., Lin, J., Zuo, M. J., & He, Z. (2014). Condition monitoring and fault diagnosis of planetary gearboxes: A review. *Measurement*, vol. 48, pp. 292-305.
- Liang, X., Zuo, M.J., & Pandey, M. (2014). Analytically evaluating the influence of crack on the mesh stiffness of a planetary gear set. *Mechanism and Machine Theory*, vol. 76, pp. 20-38.
- Liang, X., Zuo, M. J., & Hoseini, M. (2014). Understanding vibration properties of a planetary gear set for fault detection. *IEEE International Conference on Prognostics and Health Management*, June 22-25, Spokane, Washington, USA.
- Inalpolat, M., & Kahraman, A. (2009). A theoretical and experimental investigation of modulation sidebands of planetary gear sets. *Journal of Sound and Vibration*, vol. 323, pp. 677-696.
- Inalpolat, M., & Kahraman, A. (2010). A dynamic model to predict modulation sidebands of a planetary gear set having manufacturing errors. *Journal of Sound and Vibration*, vol. 329, pp. 371-393.
- Patrick, R., Ferri, A., and Vachtsevanos, G. (2012). Effect of Planetary Gear Carrier-Plate Cracks on Vibration Spectrum. *Journal of Vibration and Acoustics*, vol. 134, pp. 1- 12.
- Tian, X., Zuo, M. J. & Fyfe, K. (2004). Analysis of the vibration response of a gearbox with gear tooth faults. *Proceedings of ASME International Mechanical Engineering Congress and Exposition* (1-9). November 13-19, Anaheim, California, USA.